Algerian Journal of Engineering and Technology 02 (2020) 011–021

Algerian Journal of Engineering and Technology

Journal homepage: https://jetjournal.org/index.php/ajet

Original Article

Influence of a different fault scenarios on the properties of multi-phase induction machine

Saad Khadar[a,*]

[a]*Applied Automation and Industrial Diagnostics Laboratory, Zian Achour University, Djelfa 17000 DZ, Algeria*

ARTICLE INFO

Article history:
Received 22 November 2019
Revised 09 January 2020
Accepted 25 January 2020

Keywords:
Five phase induction motor;
Open end winding;
Turn-to-turn fault;
Power switch failures;
Open-phase fault.

ABSTRACT

This paper deals with the influence of a stator fault, power switch faults and open phase fault conditions on the properties of a five-phase induction machine under open-end stator winding (OeW-FPIM). This paper will develop an accurate mathematical model to simulate the faulty OeW-FPIM drives. The proposed model is based on the theory of electromagnetic coupling of electrical circuits coupled to the differential equation system governing the machine behavior in presence of the stator winding faults. In fact, when a short circuits between coils occurs, the stator winding function of the injured phase changes. As a consequence, the stator resistance, the stator inductance of this phase and its mutual inductance with all the other circuits change also. Consequently, the inductances and resistance matrices will be changed by taking into account the introduced coefficients of short-circuited turns. The performance of the OeW-FPIM drives have been tested via simulation under different fault scenarios conditions.

1. Introduction

The inverter-fed adjustable speed drives enable the machines drives to achieve higher drive performance, and also remove the limitation of the machine phase numbers to supply power for machines with any phase number. As a result, the multiphase machines with a phase number greater than three have been increasingly explored. This is due to their intrinsic features compared with the traditional three-phase motors like power splitting, higher torque density, reduced harmonic content of the dc-link current, improved torque quality, reduced current per phase and reduced common mode voltage etc. [1-3]. In addition, the motors with a phase number greater than three is the ability of fault tolerance where the motor able to operate in normal condition even after losing one or more phases of the stator [3]. Among different multiphase machines that have been proposed in the literature [3-5], the five-phase induction machines are probably one of the most frequently considered machines in high power applications. On the other hand, multilevel converters have some drawbacks such as dc link voltage balancing problems and use of high rating capacitors [6]. There is an alternative approach to synthesize multi-level voltage waveform is to remove the neutral from the machine and each input of stator winding is supplied by one two-level inverter [7, 8]. This topology has been investigated extensively in conjunction with three-phase drives [9-11]. However, only a few research efforts have been reported regarding multiphase motors.

Open-end winding Multiphase machines have been considered in [7, 8]. In fact, this topology offers some additional benefits such as equal power input from both sides of each winding, certain degree of fault tolerance, the possibility to eliminate common mode voltage and reducing the output voltage distortion [12-15]. However, these machines can suffer many failures. They can be electrical, mechanical or magnetic [16]. Therefore, potential defects can affect machines that will affect the safety of production, the quality of the service and the profitability of the installations if left unrecognized or

* *Corresponding author.* Tel.: 213657231202
E-mail address saadkhadar@yahoo.com
Peer review under responsibility of University of Echahid Hamma Lakhdar.
http://dx.doi.org/10.5281/zenodo.3923074

untreated. The short circuit of turns is considered the most frequent defect in the stator [17]. So, the knowledge about fault mode behavior of motor drive system is an important task to prevent the catastrophic failure of the machine. Machine modeling under fault conditions is a key to predicting its behavior [8]. In fact, an increasing research effort has been witnessed in the analysis methods of stator faults. The works in their majority is based on the signature (harmonic analysis) indicatory values such as current, torque using the theory of rotating fields and electrical circuits. So, a more precise knowledge model of the machine is necessary for an accurate analysis of the machine behavior in both healthy and faulty cases, while retaining the ability to identify the desired parameter.

On the other hand, the reliability of power electronics system such as inverter is important in high power applications. Due to frequent on-off operation the chance of failure is increased. According to recent surveys (31%-37.9%) of failure of converters are due to power switches mainly IGBT [18]. From two types of the transistor malfunctions, namely short gate-and open gate faults. These faults are mainly caused by an ageing process, which is intensified due to a thermal stress of the transistors. This paper presents an accurate model by which behavior of five-phase induction motor with open-end stator winding (OeW-FPIM) in the case of presence of stator winding faults can be successfully analyzed. Also this paper employs detailed simulations to investigate the performance of an OeW-FPIM under different fault scenarios (power switch faults and open-phase fault conditions). The remainder of the paper is organized as follows; In Section 2 presents the most common classification of faults. Section 3 represents the modeling of OeW-FPIM in presence of the faults. Then the simulation results are given in Section 4. At last the present paper ends with a conclusion.

2. The faults in electrical drives

The most common classification of faults in electrical drives defines three main groups. The power converter, the electronic sensors and the electrical machine focus the main faults in an electrical drives, as shown in Fig. 1. These faults are detailed hereafter.

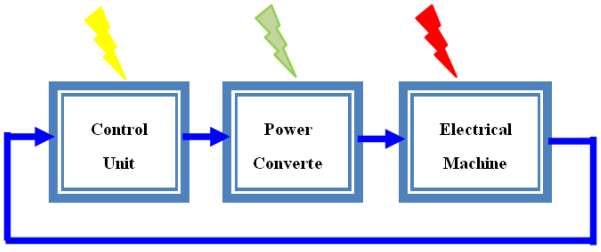

Fig. 1 Fault types of electrical drive system

2.1. Short-circuits between coils

The method followed by Siddappa and Chandrakant [10], it was adopted here on which a mixture of 2-chloro-6-methoxy-3-quinolinecarboxaldehyde (2.4g, 0.01mol) and aqueous hydrochloric acid (35cm^3, 4mol) was heated under reflux on water bath at room temperature for about 1 hour and then it was cooled to room temperature. 2-Hydroxy-6-methoxy-3-quinolinecarboxaldehyde separated as solid was collected by filtration and recrystallized from aqueous acetic acid

2.2. Open-phase fault

The open-phase fault being the most common type of fault, once an open-phase fault occurs, the originally symmetrical stator of the machine becomes asymmetrical, leading to unbalanced stator currents and voltages, the appearance of specific harmonics in the phase currents, machines vibration, noise, overheating and efficiency reduction [19-21].

2.3. Power switch failures

Faults occurring in power switches such as IGBTs and diodes can be generally classified into open gate fault and short gate fault [18], forcing the semiconductor to remain in a constant ON or OFF state.

2.3.1. Open gate transistor faults

An open gate fault occurs due to lifting of bonding wires caused by thermic cycling. An open transistor fault can lead to overstresses on the healthy transistors as well as to pulsating current. This can in turn lead to failures in other components, the line currents behave characteristically. Also, since the faulty transistor cannot conduct any current, the line current can only be positive or negative.

2.3.2. Short gate transistor faults

Short gate faults can be caused by the rupture of the connections in case of a short circuit induced overheating, by bonding wire lifting due to thermic cycling, or by a driver failure. It may be caused by a driver fault or a short-circuit-fault-induced IGBT rupture. Short transistor faults generally do not cause system shutdown, but degrade its performance.

3. Modeling of OEW-FPIM

3.1. Modeling of the FPIM

A FPIM is characterized with the spatial displacement between phases of degrees with a symmetrical squirrel-cage rotor $V_r = 0$ and $M_{sr} = M_{rs}$. The mathematical model of the five phase squirrel-cage induction motor in the original reference frame as follows [8]:

$$\begin{aligned} [V_s] &= [R_s][i_s] + [P\varphi_s] \\ [V_r] &= [0] = [R_r][i_r] + [P\varphi_r] \end{aligned} \quad (1)$$

$$\begin{aligned} [\varphi_s] &= ([M_{ss}] + [L_s])[i_s] + [M_{sr}][i_r] \\ [\varphi_r] &= [M_{rs}] + ([M_{rr}] + [L_r])[i_r^s] \end{aligned} \quad (2)$$

Where: R_s, R_r, M_{rs}, L_r, and L_s are stator resistance, rotor resistance, mutual inductance between stator and rotor, rotor cyclic inductance and stator cyclic inductance, respectively.

$$[V_s] = \begin{bmatrix} V_{sa} \\ V_{sb} \\ V_{sc} \\ V_{sd} \\ V_{se} \end{bmatrix} [V_r] = \begin{bmatrix} V_{ra} \\ V_{rb} \\ V_{rc} \\ V_{rd} \\ V_{re} \end{bmatrix}, [i_s] = \begin{bmatrix} i_{sa} \\ i_{sb} \\ i_{sc} \\ i_{sd} \\ i_{se} \end{bmatrix}, [i_r] = \begin{bmatrix} i_{ra} \\ i_{rb} \\ i_{rc} \\ i_{rd} \\ i_{re} \end{bmatrix} : \text{represent}$$

the five-phase stator and rotor voltage vectors, the five-phase stator and rotor current vectors, respectively.

$$[\varphi_s] = \begin{bmatrix} \varphi_{sa} \\ \varphi_{sb} \\ \varphi_{sc} \\ \varphi_{sd} \\ \varphi_{se} \end{bmatrix}, [\varphi_r] = \begin{bmatrix} \varphi_{ra} \\ \varphi_{rb} \\ \varphi_{rc} \\ \varphi_{rd} \\ \varphi_{re} \end{bmatrix} :$$

Are the five-phase stator and rotor flux linkages, respectively.

3.2. Open winding inverter configuration

Figure.2, presents the circuit principle of the studied topology in this paper [7, 8, 22-24], where only one DC source is used to provide the required input power to the dual inverter feeding the OeW-FPIM drive. The two inverters are marked by indices 1 and 2, while the inverter 1 is connected to stator winding terminal of a1, b1, c1, d1 and e1 and inverter 2 is connected to stator winding terminal of a2, b2, c2, d2 and e2. By using this structure, the inverters can be operated as a two-level, three-level or four-level inverter (see Fig. 3), without the need to change the structure of the inverter.

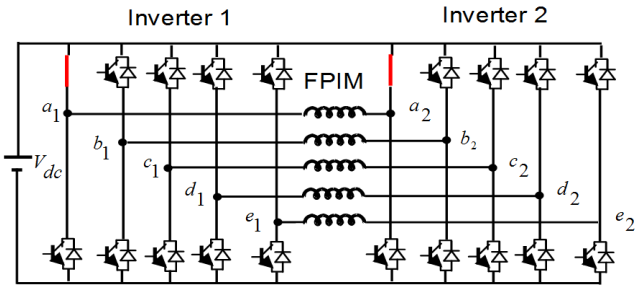

Fig. 2 Five phase induction motor open-end winding

According to Fig. 2 the phase voltages across each stator winding can be obtained by applying Kirchhoff's law as follows:

$$\begin{cases} V_{sa} = V_{a10} - V_{a20} \\ V_{sb} = V_{b10} - V_{b20} \\ V_{sc} = V_{c10} - V_{c20} \\ V_{sd} = V_{d10} - V_{d20} \\ V_{se} = V_{e10} - V_{e20} \end{cases}$$

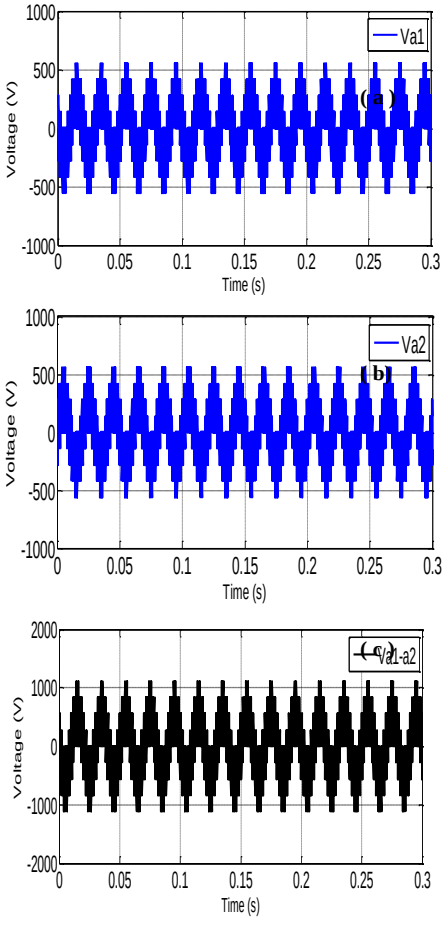

Fig. 3. - (a) the output voltages of the inverter 1; (b) the output voltages of the inverter 2; (c) the output voltages of the two inverters

3.2. Modeling of the FPIM in the presence of stator faults

A FPIM with stator winding fault at (a1-a2) phase is shown in Fig. 4 [8], where represents the number of turns in short circuit in phase (a1-a2) and is the number of turns in the healthy state. The modeling method of the FPIM is based on the theory of electromagnetic coupling of electrical circuits. We get the new five phase model which represents the model of the FPIM in the presence of stator faults in first phase as [8]:

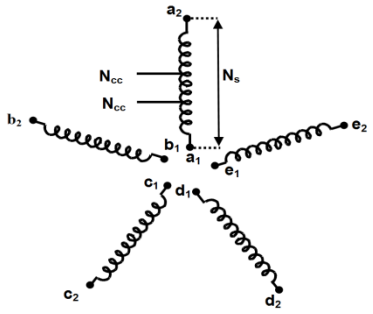

Fig. 4 Stator winding scheme with a short-circuits fault between coils.

$$\begin{cases}
\frac{di_{sa}}{dt} = U_{SA} + A_1 i_{sa} + A_2 i_{sb} + A_3 i_{sc} + A_4 i_{sd} + A_5 i_{se} + k f_{sa} f_{sb}^2 f_{sc}^2 f_{sd}^2 f_{se}^2 \left(\mathrm{G}\,\varphi_{sa} + G_1 \varphi_{sb} - G_2 \varphi_{sc} + G_1 \varphi_{sd} - G_2 \varphi_{se} \right) \\
\frac{di_{sb}}{dt} = U_{SB} + B_1 i_{sa} + B_2 i_{sb} + B_3 i_{sc} + B_4 i_{sd} + B_5 i_{se} + k f_{sa}^2 f_{sb} f_{sc}^2 f_{sd}^2 f_{se}^2 \left(-G_2 \varphi_{sa} + \mathrm{G}\,\varphi_{sb} + G_1 \varphi_{sc} - G_2 \varphi_{sd} + G_1 \varphi_{se} \right) \\
\frac{di_{sc}}{dt} = U_{SC} + C_1 i_{sa} + C_2 i_{sb} + C_3 i_{sc} + C_4 i_{sd} + C_5 i_{se} + k f_{sa}^2 f_{sb}^2 f_{sc} f_{sd}^2 f_{se}^2 \left(G_1 \varphi_{sa} - G_2 \varphi_{sb} + \mathrm{G}\,\varphi_{sc} + G_1 \varphi_{sd} - G_2 \varphi_{se} \right) \\
\frac{di_{sd}}{dt} = U_{SD} + D_1 i_{sa} + D_2 i_{sb} + D_3 i_{sc} + D_4 i_{sd} + D_5 i_{se} + k f_{sa}^2 f_{sb}^2 f_{sc}^2 f_{sd} f_{se}^2 \left(-G_2 \varphi_{sa} + G_1 \varphi_{sb} - G_2 \varphi_{sc} + G\,\varphi_{sd} + G_1 \varphi_{se} \right) \\
\frac{di_{se}}{dt} = U_{SE} + E_1 i_{sa} + E_2 i_{sb} + E_3 i_{sc} + E_4 i_{sd} + E_5 i_{se} + k f_{sa}^2 f_{sb}^2 f_{sc}^2 f_{sd}^2 f_{se} \left(G_1 \varphi_{sa} - G_2 \varphi_{sb} + G_1 \varphi_{sc} - G_2 \varphi_{sd} + G\,\varphi_{se} \right)
\end{cases} \quad (4)$$

$$\begin{cases}
\frac{d\varphi_{ra}}{dt} = \lambda \left(f_{sa} i_{sa} - \frac{f_{sb} i_{sb}}{2} - \frac{f_{sc} i_{sd}}{2} - \frac{f_{sd} i_{sd}}{2} - \frac{f_{se} i_{se}}{2} \right) - k_{A1} \varphi_{ra} - k_{A2} \varphi_{rb} - k_{A3} \varphi_{rc} - k_{A2} \varphi_{rd} - k_{A3} \varphi_{re} \\
\frac{d\varphi_{rb}}{dt} = \lambda \left(-\frac{f_{sa} i_{sa}}{2} + f_{sb} i_{sb} - \frac{f_{sc} i_{sc}}{2} - \frac{f_{sd} i_{sd}}{2} - \frac{f_{se} i_{se}}{2} \right) - k_{A3} \varphi_{ra} - k_{A1} \varphi_{rb} - k_{A2} \varphi_{rc} - k_{A3} \varphi_{rd} - k_{A2} \varphi_{re} \\
\frac{d\varphi_{rc}}{dt} = \lambda \left(-\frac{f_{sa} i_{sa}}{2} - \frac{f_{sb} i_{sb}}{2} + f_{sc} i_{sc} - \frac{f_{sd} i_{sd}}{2} - \frac{f_{se} i_{se}}{2} \right) + -k_{A2} \varphi_{ra} - k_{A3} \varphi_{rb} - k_{A1} \varphi_{rc} - k_{A2} \varphi_{rd} - A_3 \varphi_{re} \\
\frac{d\varphi_{rd}}{dt} = \lambda \left(-\frac{f_{sa} i_{sa}}{2} - \frac{f_{sb} i_{sb}}{2} - \frac{f_{sc} i_{sc}}{2} + f_{sd} i_{sd} - \frac{f_{se} i_{se}}{2} \right) + -k_{A3} \varphi_{ra} - k_{A2} \varphi_{rb} - k_{A3} \varphi_{rc} - k_{A1} \varphi_{rd} - k_{A2} \varphi_{re} \\
\frac{d\varphi_{re}}{dt} = \lambda \left(-\frac{f_{sa} i_{sa}}{2} - \frac{f_{sb} i_{sb}}{2} - \frac{f_{sc} i_{sc}}{2} - \frac{f_{sd} i_{sd}}{2} + f_{se} i_{se} \right) + -k_{A2} \varphi_{ra} - k_{A3} \varphi_{rb} - k_{A2} \varphi_{rc} - k_{A3} \varphi_{rd} - k_{A1} \varphi_{re}
\end{cases} \quad (5)$$

The electromagnetic torque is determined by:

$$\begin{aligned}
& J \frac{d\Omega}{dt} + F\Omega = T_e - T_L \\
& T_e = p \frac{M_{sr}}{L_r} \left([I_s] \wedge [\varphi_r] \right)
\end{aligned} \quad (6)$$

Where: p : is the number of pole pairs. T_L : is the load torque. J : is the moment of inertia and F : is the friction coefficient.

4. Simulation results

In order to investigate the influence of a stator fault, power switch faults and open phase fault conditions on the properties of a five-phase induction machine under open-end stator winding, a some numerical simulation have been

conducted by using MATLAB/SIMULINK. The performance of OeW-FPIM drive has been tested in several operating conditions such as the following: healthy operation and faulty operation. In addition, a very simple modulation control strategy is chosen for this studied topology, i.e. a Sinusoidal pulse width modulation (SPWM) strategy, which requires a triangle waveform and a comparator. The simulation results have been obtained with no load and the load is changed to 5 N. m at t=1s.

4.1 System performance under short-circuit between coils

The topology of the OeW-FPIM is given in Fig. 5, with a short-circuit between coils fault of the first phase (a1-a2) With regard to the faults of short-circuit between coils, two types of failures were introduced, where $N_{cc}=50$ and $N_{cc}=100$ the turns in short- circuit, therefore we will have respectively $N_1=150$ and $N_1=100$ turns that phase will be useful, $N_s=200$ the number of turns in healthy operation.

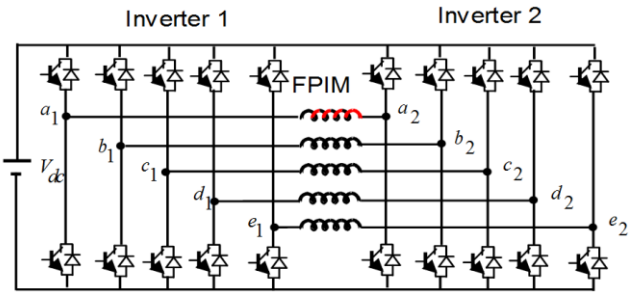

Fig. 5 The topology of the OeW-FPIM drive under short-circuit between coils

The waveforms of the rotor speed, the electromagnetic torque and the five phase stator currents at various load and fault conditions are presented in Fig. 6. From these results, it can be observed that the speed and torque values decreases slightly and oscillates after the fault occurrence at 1.5 s. The appearance of these oscillations is directly related to the existence of a residual asymmetry in the motor stator circuit (seen Fig. a6).

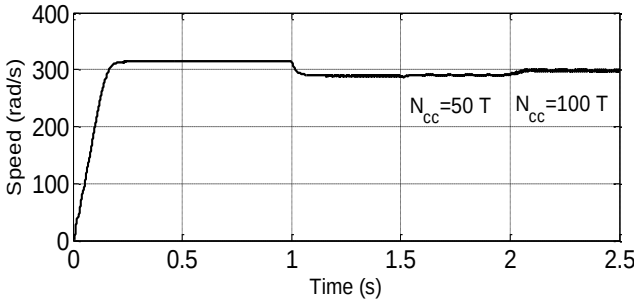

(a)

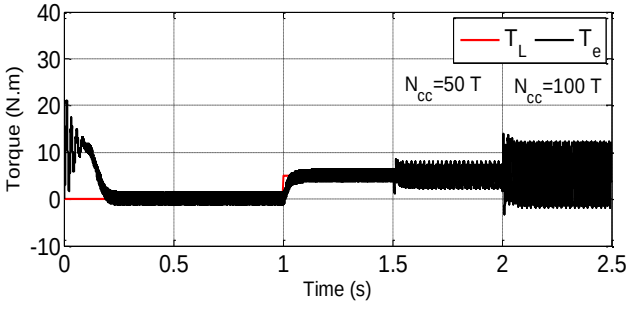

(b)

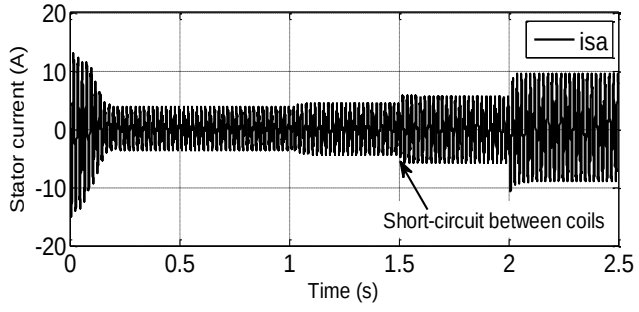

(c)

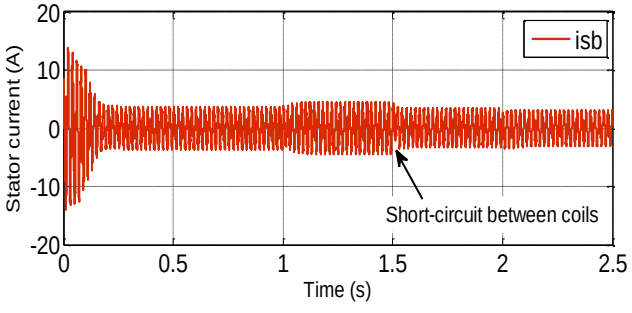

(d)

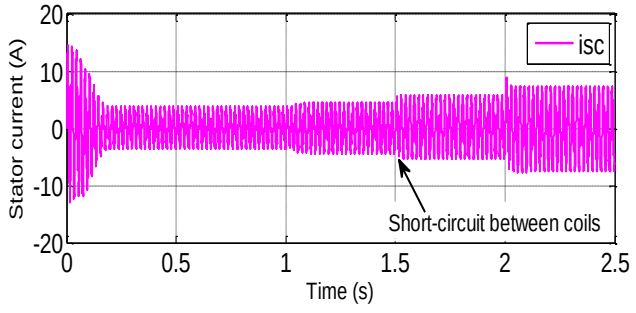

(e)

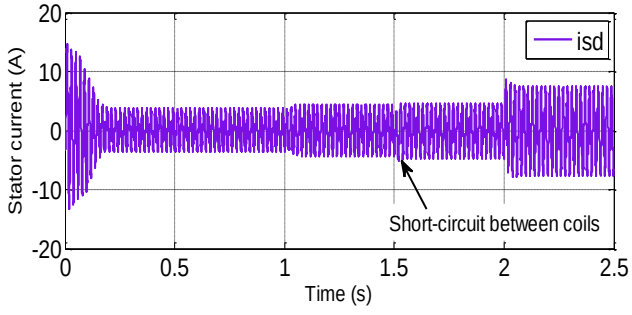

(f)

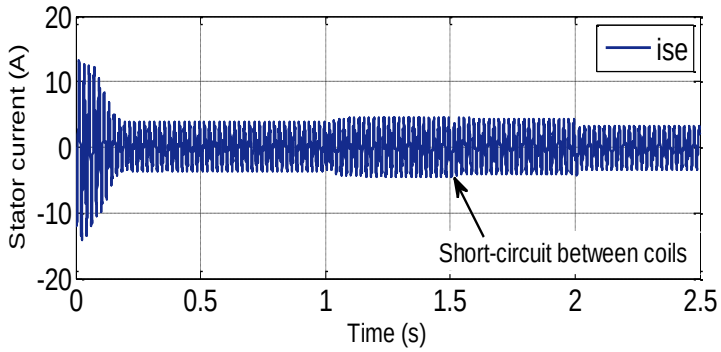

(g)

Fig. 6 Simulation results of the OeW-FPIM derive under short-circuit between coils - (a) the rotor speed; (b) the torque; (c) the a-phase current; (d) the b-phase current; (e) the c-phase current; (f) the d-phase current; (g) the e-phase current

Figure. b6 shows the electromagnetic torque of the machine, it can be seen that the developed torque presents fast dynamic with good response, where it tracks precisely the imposed step changes of the load torque. Fig. c6 to Fig. g6, it can be noted that the stator current (a1-a2) after the fault occurrence, increases considerably compared to the healthy case. This increase is related to the number of coils in short-circuit. This is obviously the simultaneous decrease of resistance and the inductance phase of the stator winding.

4.2 System performance under power switch faults

4.2.1 Open gate transistor faults

The topology of the OeW-FPIM is given in Fig. 7, with an open gate transistor fault of the upper switch (S1) of the first inverter and an open gate transistor fault of the upper switch (S6) of the second inverter. To analyze the faulty IGBT's impact on OeW-FPIM drive, let's consider Fig. 8.

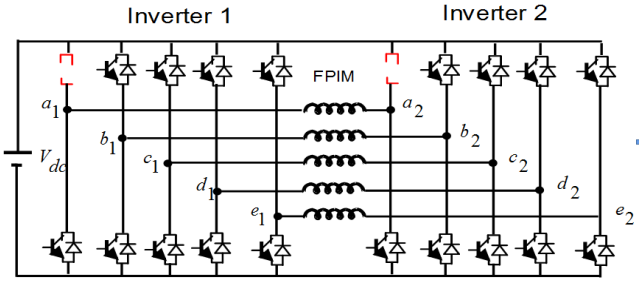

Fig. 7 The topology of the OeW-FPIM drive under open gate transistor faults

The waveforms of the rotor speed, the electromagnetic torque and the five phase stator currents in the case that the gate transistor is open at load conditions are presented in Fig. 8. From the Fig. a8, it can be noted that the speed is gradually reduced to around 92% of the rotor speed when gate transistor (S1 and S2) is open. Fig. b8 shows the electromagnetic torque, it can be observed a disturbance at the electromagnetic torque of OeW-FPIM, while the five phase stator currents is not balanced any more as plotted in Fig. c8 to Fig. g8.

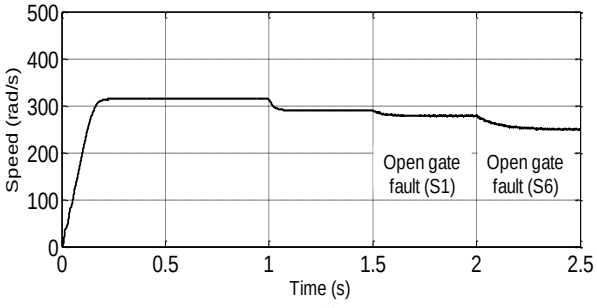

(a)

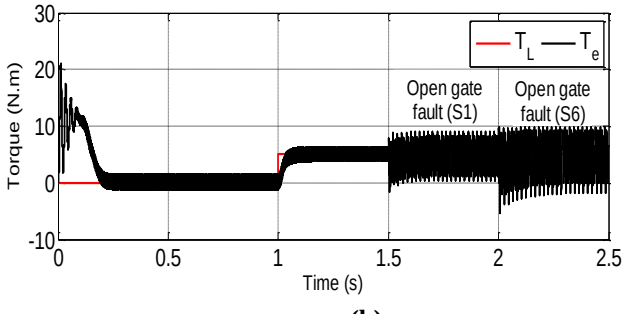

(b)

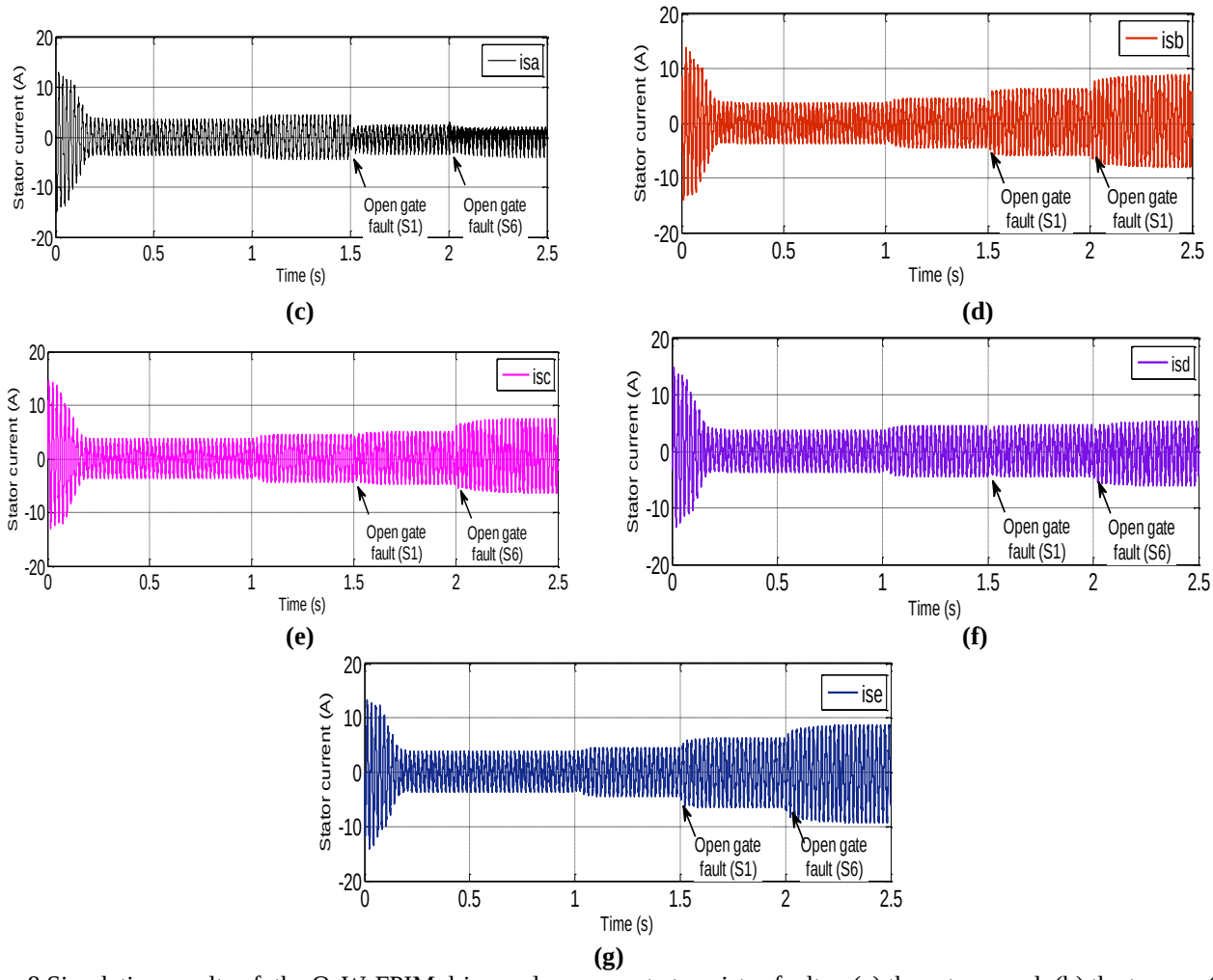

Fig. 8 Simulation results of the OeW-FPIM drive under open gate transistor faults - (a) the rotor speed; (b) the torque; (c) the a-phase current; (d) the b-phase current; (e) the c-phase current; (f) the d-phase current; (g) the e-phase current

4.2.2 Short gate transistor faults

The topology of the OeW-FPIM is given in Fig. 9, with a short gate transistor fault of the upper switch (S1) of the first inverter and a short gate transistor fault of the upper switch (S6) of the second inverter. To analyze the faulty IGBT's impact on the OeW-FPIM drive, let's consider Fig. 10.

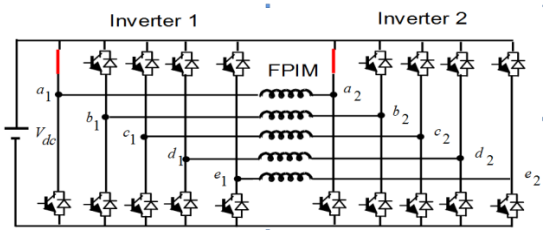

Fig. 9 The topology of the OeW-FPIM drive under short gate transistor faults

The waveforms of the rotor speed, the electromagnetic torque and the five phase stator currents in the case that the gate transistor is short at load conditions are presented in Fig. 10. As can be seen, the torque fluctuations is 2.4 N.m under the healthy condition. When the short circuit fault occur, the torque fluctuations is 4.7 N.m (seen Fig. a10). In fact, these cause fluctuations of the rotor speed, which generates acoustic noise and thus, an abnormal operation of the motor. The five phase stator currents are shown in Fig. c10 to Fig. g10, it can be observed the remaining phase currents are increased when the gate transistor (S1 and S2) are short.

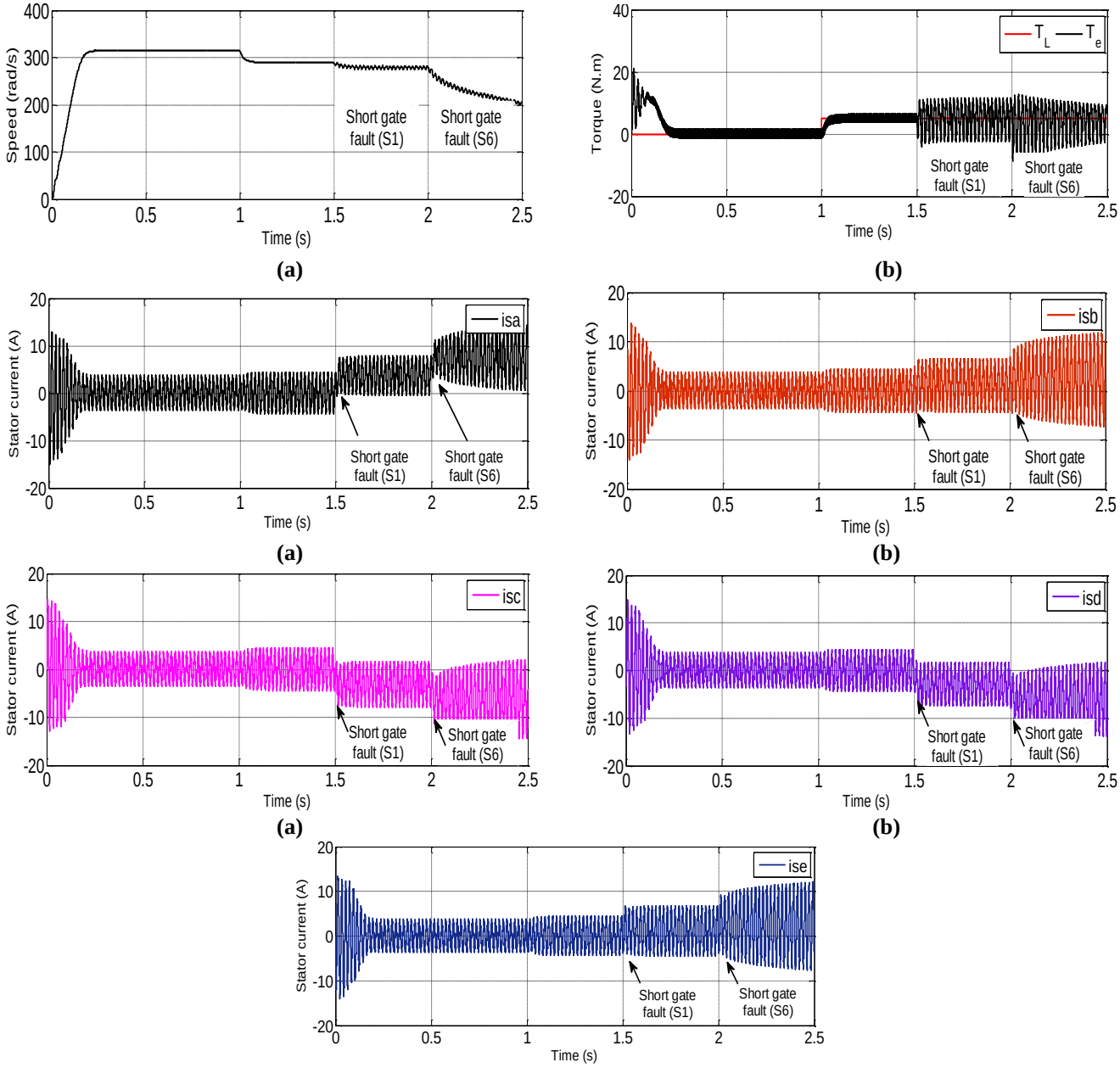

Fig. 10 Simulation results of the OeW-FPIM drive under short gate transistor faults - (a) the rotor speed; (b) the torque; (c) the a-phase current; (d) the b-phase current; (e) the c-phase current; (f) the d-phase current; (g) the e-phase current

4.3 System performance under open-phase fault

The topology of the OeW-FPIM is given in Fig. 11, with

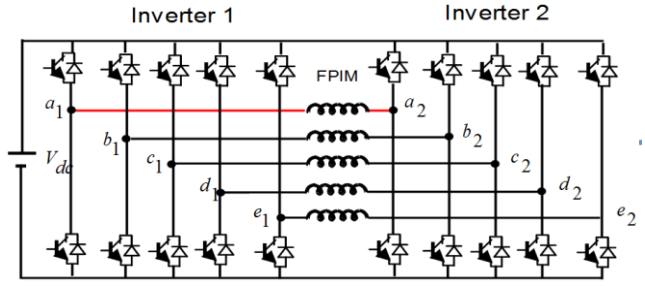

Fig. 11 The topology of the OeW-FPIM drive under open-phase fault

open-phase fault of the first phase (a1-a2). To analyze the open-phase fault impact on the OeW-FPIM drive, let's consider Fig. 12.

The waveforms of the rotor speed, the electromagnetic torque and the five phase stator currents in the case that the open-phase faults at load conditions are presented in Fig. 12. From the Fig. a12, it can be noted that the speed is gradually reduced to around 95% of the rotor speed when the phase (a1-a2) is open, Fig. b12 shows the electromagnetic torque, it can be observed an oscillations at the electromagnetic torque, while the five phase stator currents is not balanced any more after the fault occurrence as shown in Fig. c12 to Fig. g12.

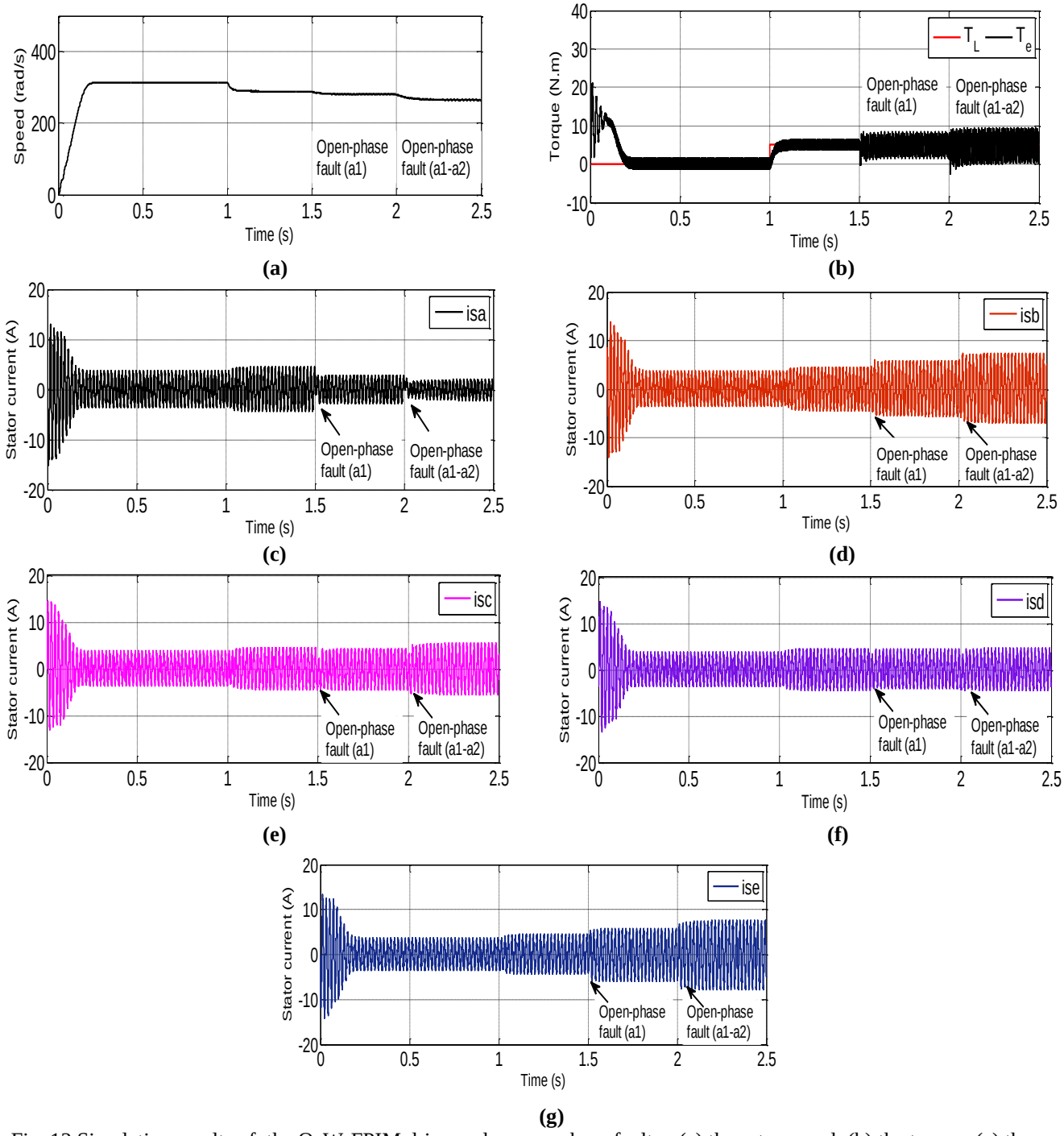

Fig. 12 Simulation results of the OeW-FPIM drive under open-phase faults - (a) the rotor speed; (b) the torque; (c) the a-phase current; (d) the b-phase current; (e) the c-phase current; (f) the d-phase current; (g) the e-phase current

Finally, the proposed method of modeling for the OeW-FPIM drive under short circuit fault between coils is different from the previous published works [25-28], where, the proposed method is based mainly on the motor parameters that change during the stator winding faults. Adopting such a model can provide a more accurate representation of the machine behavior in both healthy and faulty cases. This fault model is based on a simple equations in comparison with the works presented in [25-28], which ensures more simplification. On the other hand, the study of the impact of these different fault scenarios is an original application where it is applied in this paper for the first time of the studied topology.

5. Conclusion

The objective of the proposed idea in this paper is to analyze behavior of five-phase induction motor with open-end stator winding supplied by two converters under a stator fault, power switch faults and open-phase fault conditions. Firstly, this paper presents a mathematical model by which behavior of OeW-FPIM with short circuit between coils in the stator winding can be analyzed. Second, the obtained results confirm that the proposed mathematical model allows showing the effect of this fault for the OeW-FPIM topology. Such this fault model can be further used in fault-tolerant strategies or for precise diagnostic purposes. For this purpose, our next objective will be to detect and diagnostic the faults of short circuit between coils and a fault tolerant strategy will be implemented to control the OeW-FPIM topology using parameters estimation. Fault tolerant control aims in ensuring the continuous operation of the system under a degraded mode.

References

1. Pieńkowski K. Analysis and control of dual stator winding induction motor. *Archives of Electrical Engineering*. 2012;61(3):421-438. https://doi.org/10.2478/v10171-012-0033-z.
2. Duran MJ, Barrero F. Recent advances in the design, modeling, and control of multiphase machines—Part II. IEEE Transactions on Industrial Electronics. 2015;63(1):459-468.https://doi.org/10.1109/TIE.2015.2448211.
3. Barrero F, Duran MJ. Recent advances in the design, modeling, and control of multiphase machines—Part I. *IEEE Transactions on Industrial Electronics*. 2015;63(1):449-458. https://doi.org/10.1109/TIE.2015.2447733.
4. Abdel-Khalik AS, Masoud MI, Williams BW. Improved flux pattern with third harmonic injection for multiphase induction machines. *IEEE Transactions on Power Electronics*. 2011;27(3):1563-1578. https://doi.org/10.1109/TPEL.2011.2163320.
5. Mengoni M, Zarri L, Tani A, Gritli Y, Serra G, Filippetti F, Casadei D. Online detection of high-resistance connections in multiphase induction machines. *IEEE Transactions on Power Electronics*. 2014;30(8):4505-13.. https://doi.org/10.1109/TPEL.2014.2357439.
6. de Lillo L, Empringham L, Wheeler PW, Khwan-On S, Gerada C, Othman MN, Huang X. Multiphase power converter drive for fault-tolerant machine development in aerospace applications. *IEEE Transactions on Industrial Electronics*. 2009;57(2):575-583. https://doi.org/10.1109/TIE.2009.2036026.
7. Saad K, Abdellah K, Ahmed H, Iqbal A. Investigation on SVM-Backstepping sensorless control of five-phase open-end winding induction motor based on model reference adaptive system and parameter estimation. *Engineering Science and Technology, an International Journal*. 2019;22(4):1013-1026.. https://doi.org/10.1016/j.jestch.2019.02.008.
8. Khadar S, Kouzou A, Rezzaoui MM, Hafaifa A. Sensorless control technique of open-end winding five phase induction motor under partial stator winding short-circuit. *Periodica Polytechnica Electrical Engineering and Computer Science*. 2020;64(1):2-19. https://doi.org/10.3311/PPee.14306.
9. Chowdhury S, Wheeler PW, Patel C, Gerada C. A multilevel converter with a floating bridge for open-end winding motor drive applications. *IEEE Transactions on Industrial Electronics*. 2016;63(9):5366-5375. https://doi.org/10.1109/TIE.2016.2561265.
10. Jacobina CB, Oliveira AC, de Almeida Carlos GA, de Rossiter Corrêa MB. Hybrid modular multilevel DSCC inverter for open-end winding induction motor drives. *IEEE Transactions on Industry Applications*. 2016;53(2):1232-1242. https://doi.org/10.1109/TIA.2016.2632701.
11. Sekhar KR, Srinivas S. Discontinuous decoupled PWMs for reduced current ripple in a dual two-level inverter fed open-end winding induction motor drive. *IEEE Transactions on Power Electronics*. 2012;28(5):2493-2502. https://doi.org/10.1109/TPEL.2012.2215344.
12. Jones M, Satiawan IN, Bodo N, Levi E. A dual five-phase space-vector modulation algorithm based on the decomposition method. *IEEE Transactions on Industry Applications*. 2012;48(6):2110-2120. https://doi.org/10.1109/TIA.2012.2226422.
13. Riedemann J, Clare JC, Wheeler PW, Blasco-Gimenez R, Rivera M, Pena R. Open-end winding induction machine fed by a dual-output indirect matrix converter. *IEEE Transactions on Industrial Electronics*. 2016;63(7):4118-4128.. https://doi.org/10.1109/TIE.2016.2531020.
14. Kalaiselvi J, Srinivas S. Bearing currents and shaft voltage reduction in dual-inverter-fed open-end winding induction motor with reduced CMV PWM methods. *IEEE Transactions on Industrial Electronics*. 2014;62(1):144-52. https://doi.org/10.1109/TIE.2014.2336614.
15. Wang Y, Panda D, Lipo TA, Pan D. Open-winding power conversion systems fed by half-controlled converters. *IEEE Transactions on Power Electronics*. 2012;28(5):2427-2436. https://doi.org/10.1109/TPEL.2012.2218259.
16. Nandi S, Toliyat HA, Li X. Condition monitoring and fault diagnosis of electrical motors—A review. *IEEE transactions on energy conversion*. 2005;20(4):719-729. https://doi.org/10.1109/TEC.2005.847955.
17. Siddique A, Yadava GS, Singh B. A review of stator fault monitoring techniques of induction motors. *IEEE transactions on energy conversion*. 2005 Feb 22;20(1):106-114. https://doi.org/10.1109/TEC.2004.837304.
18. Bae CJ, Lee DC, Nguyen TH. Detection and identification of multiple IGBT open-circuit faults in PWM inverters for AC machine drives. *IET Power Electronics*. 2019;12(4):923-931. https://dx.doi.org/10.1049/iet-pel.2018.5188.
19. Guzman H, Duran MJ, Barrero F, Bogado B, Toral S. Speed control of five-phase induction motors with integrated open-phase fault operation using model-based predictive current control techniques. *IEEE Transactions on Industrial Electronics*. 2013 Nov 8;61(9):4474-4484. https://doi.org/10.1109/TIE.2013.2289882.

20. Schreier L, Bendl J, Chomat M. Operation of five-phase induction motor after loss of one phase of feeding source. *Electrical Engineering*. 2017;99(1):9-18. https://doi.org/10.1007/s00202-016-0370-9.
21. Zhou H, Zhao W, Liu G, Cheng R, Xie Y. Remedial field-oriented control of five-phase fault-tolerant permanent-magnet motor by using reduced-order transformation matrices. *IEEE Transactions on Industrial Electronics*. 2016;64(1):169-178. https://doi.org/10.1109/TIE.2016.2599501.
22. Listwan J, Pieńkowski K. Field-oriented control of five-phase induction motor with open-end stator winding. *Archives of Electrical Engineering*. 2016;65(3). https://doi.org/10.1515/aee-2016-0029.
23. Satiawan IN, Citarsa IB, Wiryajati IK, Aware MV. Performance comparison of PWM schemes of dual-inverter fed five-phase motor drives. *International Journal of Technology*. 2014;5(3):277-286. https://doi.org/10.14716/ijtech.v5i3.609.
24. Bodo N, Jones M, Levi E. A space vector PWM with common-mode voltage elimination for open-end winding five-phase drives with a single DC supply. *IEEE Transactions on Industrial Electronics.* 2014;61(5):2197-2207.. https://doi.org/10.1109/TIE.2013.2272273.
25. Devanneaux V, Dagues B, Faucher J, Barakat G. An accurate model of squirrel cage induction machines under stator faults. *Mathematics and computers in simulation*. 2003;63(3-5):377-391. https://doi.org/10.1016/S0378-4754(03)00083-1.
26. Leboeuf N, Boileau T, Nahid-Mobarakeh B, Takorabet N, Meibody-Tabar F, Clerc G. Estimating permanent-magnet motor parameters under inter-turn fault conditions. *IEEE transactions on magnetics*. 2012;48(2):963-966. https://doi.org/10.1109/TMAG.2011.2177642.
27. Soufi Y, Bahi T, Merabet H, Lekhchine S. Short circuit between turns in stator winding of induction machine fault detection and diagnosis. InApplied mechanics and materials 2013 (Vol. 416, pp. 565-571). Trans Tech Publications Ltd. https://doi.org/10.4028/www.scientific.net/AMM.416-417.565.
28. Guezmil A, Berriri H, Pusca R, Sakly A, Romary R, Mimouni MF. Detecting inter-turn short-circuit fault in induction machine using high-order sliding mode observer: simulation and experimental verification. *Journal of Control, Automation and Electrical Systems.* 2017;28(4):532-540. https://doi.org/10.1007/s40313-017-0314-2.

Recommended Citation

Khadar S. Influence of a Different Fault Scenarios on the Properties of Multi-Phase Induction Machine. *Alg. J. Eng. Tech.* 2020; 2: 011-021. http://dx.doi.org/10.5281/zenodo.3923074